*Free Radical Research*, June 2010; 44(6): 694–709

informa
healthcare

# Modulation of inflammatory response after spinal cord trauma with deferoxamine, an iron chelator

IRENE PATERNITI[1], EMANUELA MAZZON[2], ESPOSITO EMANUELA[1,2], ROSANNA DI PAOLA[2], MARIA GALUPPO[1], PLACIDO BRAMANTI[2] & SALVATORE CUZZOCREA[1,2]

[1]*Department of Clinical and Experimental Medicine and Pharmacology, School of Medicine, Messina, Italy, and* [2]*IRCCS Centro Neurolesi 'Bonino-Pulejo', Messina, Italy*

*(Received date: 14 January 2010; In revised form date: 22 February 2010)*

**Abstract**

The standard iron-chelator deferoxamine is known to reduce neurological deficits. The aim of the present study was to evaluate the contribution of deferoxamine in the secondary damage in experimental spinal cord injury (SCI) in mice, induced by the application of vascular clips to the dura via a four-level T5–T8 laminectomy. SCI resulted in production of inflammatory mediators, tissue damage and apoptosis. Deferoxamine treatment 30 min before and 1 and 6 h after the SCI significantly reduced: (1) GFAP immunoreactivity, (2) neutrophil infiltration, (3) NF-κB activation, (4) iNOS expression, (5) nitrotyrosine and MDA formation, (6) DNA damage (methyl green pyronin staining and PAR formation and (7) apoptosis (TUNEL staining, FasL, Bax and Bcl-2 expression, S-100 expression). Moreover, deferoxamine significantly ameliorated the recovery of limb function (evaluated by motor recovery score). Taken together, the results clearly demonstrate that deferoxamine treatment reduces the development of inflammation and tissue injury associated with spinal cord trauma.

**Keywords:** *SCI, inflammatory mediators, tissue damage, apoptosis.*

## Introduction

Spinal cord injury (SCI) usually leads to devastating neurological deficits and disabilities. Complete spinal cord injury is irreversible. Muscle power and sensation is lost, leading to spasticity, pressure ulcers, neurogenic pain and restricted activities of daily living and mobility.

Recently, the National Spinal Cord Injury Statistical Center reported that the annual incidence of SCI in the US is estimated to be 40 cases per million people [1]. People with traumatic SCI are at greater risk than the general population throughout their lifetime for medical complications that may necessitate re-hospitalization.

The contemporary management of SCI consists of supportive care and stabilization of the spine [2]. Several mechanisms are involved in injury after trauma, including microvascular dysfunction at the site of injury [3], free radicals formation and lipid peroxidation and accumulation of excitatory neurotransmitters, e.g. glutamate (acting on N-methyl-D-aspartate [NMDA] and non-NMDA receptors), leading to neural damage due to excessive excitation (excitotoxicity), depletion of high energy metabolites, leading to anaerobic metabolism at the site of injury, provocation of an inflammatory response and recruitment and activation of inflammatory cells associated with secretion of cytokines, which contribute to further tissue damage [4], and activation of calpains and caspases, leading to cellular apoptosis [5].

It's known that, after SCI, the levels of free iron are also increased quickly [6]. Iron plays an important role in glutamate excitotoxicity in spinal cord motor neurons which suggests that lowering tissue iron level alone may be an effective and sufficient strategy for protection against glutamate excitotoxicity [7]. Yu et al. [7] have clearly showed that iron chelator Deferoxamine (DFO) mesylate completely prevented

Correspondence: Professor Salvatore Cuzzocrea, Department of Clinical and Experimental Medicine and Pharmacology, School of Medicine, University of Messina, Torre Biologica, Policlinico Universitario Via C. Valeria, Gazzi, 98100 Messina, Italy. Tel: (39) 090 2213644. Fax: (39) 090 2213300. Email: salvator@unime.it

ISSN 1071-5762 print/ISSN 1029-2470 online 
DOI: 10.3109/10715761003742993

the neurotoxic effects of threohydroxyaspartate, which is an inhibitor of glutamate transport and causes glutamate excitotoxicity. The major sources of iron accumulation in the brain are iron in the plasma and haemoglobin after erythrocyte lysis.

DFO is the current standard for iron chelation therapy. DFO was the first commercially-available Fe chelator to be assessed in cancer therapy, where, for example, it was shown to reduce bone marrow infiltration of tumour cells in seven of nine neuroblastoma patients [8].

Although DFO has some anti-proliferative activity, it suffers serious limitations [9]. It is highly hydrophilic, orally inactive, has poor membrane permeability and is expensive to produce [9]. It also possesses a very short half-life in plasma (5–10 min) due to rapid metabolism [9]. Otherwise the purpose of this drug is as a therapeutic for Fe overload. It has been demonstrated that DFO can attenuate acute brain oedema and oxidative stress following intracerebral haemorrhage, although the time course of free iron accumulation after intracerebral haemorrhage is unknown [10].

We have, therefore, carried out investigations to determine the possible beneficial effects of iron chelator DFO on an experimental model of spinal cord trauma in mice.

In particular to gain a better insight into the mechanism(s) of action of DFO, we evaluated the following end-points of the inflammatory response: (1) histological damage, (2) motor recovery, (3) neutrophil infiltration, (4) NF-κB activation, (5) nitrotyrosine and poly-ADP-ribose (PAR) formation, (6) pro-inflammatory cytokine production, (7) inducible nitric oxide synthase (iNOS) expression, (8) apoptosis as TUNEL staining and (9) Bax and Bcl-2 expression.



## Materials and methods

### *Animals*

Male Adult CD1 mice (25–30 g, Harlan Nossan, Milan, Italy) were housed in a controlled environment and provided with standard rodent chow and water. Animal care was in compliance with Italian regulations on protection of animals used for experimental and other scientific purposes (D.M. 116192) as well as with the EEC regulations (O.J. of E.C. L 358/1 12/18/1986).

### *SCI*

Mice were anaesthetized using chloral hydrate (400 mg/kg body weight). A longitudinal incision was made on the mid-line of the back, exposing the paravertebral muscles. These muscles were dissected away exposing T5–T8 vertebrae. The spinal cord was exposed via a four-level T5–T8 laminectomy and SCI was produced by extradural compression of the spinal cord using an aneurysm clip with a closing force of 24 g. Following surgery, 1.0 cc of saline was administered subcutaneously in order to replace the blood volume lost during the surgery. During recovery from anaesthesia, mice were placed on a warm heating pad and covered with a warm towel. Mice were singly housed in a temperature-controlled room at 27°C for a survival period of 10 days. Food and water were provided to the mice *ad libitum*. During this time period, the animals' bladders were manually voided twice a day until the mice were able to regain normal bladder function. In all injured groups, the spinal cord was compressed for 1 min. Sham animals were only subjected to laminectomy.

### *Experimental design*

Mice were randomly allocated into the following groups:

i) *SCI+vehicle group*. Mice were subjected to SCI plus administration of saline (administered i.p., 30 min before and 1 h and 6 h after SCI) ($n=40$);
ii) *DFO group*. Same as the *SCI+vehicle group* but in which DFO (30 mg/kg) was administered i.p., 30 min before and 1 h and 6 h after SCI ($n=40$);
iii) *Sham+vehicle group*. Mice were subjected to the surgical procedures as the above groups except that the aneurysm clip was not applied and to these mice was administered saline (administered i.p., 30 min before and 1 h and 6 h, after SCI) ($n=40$);
iv) *Sham+DFO group*. Identical to *Sham+vehicle group* except for the administration of DFO (30 mg/kg administered i.p., 30 min before and 1 h and 6 h after SCI) ($n=40$).

As described below mice ($n=10$ from each group for each parameters) were sacrificed at 24 h after SCI in order to evaluate the various parameter. In a separate set of experiments another 10 animals for each group were observed until 10 days after SCI in order to evaluate the motor score. The doses of DFO (30 mg/kg) used here were based on previous *in vivo* study [11].

### *Light microscopy*

Spinal cord biopsies were taken at 24 h following trauma. Tissue segments containing the lesion (1 cm on each side of the lesion) were paraffin embedded and cut into 5-μm-thick sections. Tissue longitudinal sections (thickness 5 μm) were deparaffinized with xylene, stained with Haematoxylin/Eosin (H&E), with methyl green pyronin staining (used to simultaneously DNA and RNA), with silver impregnation for reticulum and studied using light microscopy (Dialux 22 Leitz, Milan, Italy).

The segments of each spinal cord were evaluated in the rostral/caudal perilesional area by an experienced histopathologist (RO). Damaged neurons were counted and the histopathologic changes of the gray matter were scored on a six-point scale [12]: 0, no lesion observed, 1, gray matter contained 1–5 eosinophilic neurons; 2, gray matter contained 5–10 eosinophilic neurons; 3, gray matter contained more than 10 eosinophilic neurons; 4, small infarction (less than one third of the gray matter area); 5, moderate infarction (one third to one half of the gray matter area); and 6, large infarction (more than half of the gray matter area). The scores from all the sections from each spinal cord were averaged to give a final score for individual mice. All the histological studies were performed in a blinded fashion.

*Myeloperoxidase activity*

Myeloperoxidase (MPO) activity, an indicator of polymorphonuclear leukocyte (PMN) accumulation, was determined in the spinal cord tissues as previously described [13] at 24 h after SCI. MPO activity was defined as the quantity of enzyme degrading 1 μmol of peroxide min-$^{1}$ at 37°C and was expressed in units/g of wet tissue.

*MDA measurement*

The levels of MDA in the intestinal tissues were determined as an indicator of lipid peroxidation [14]. After 120 min of reperfusion, intestinal tissues were removed, weighed and homogenized in 1.15% (w/v) KCl solution. An aliquot (100 μl) of the homogenate was added to a reaction mixture containing 200 μl of 8.1% (w/v) sodium dodecyl sulphate, 1500 μl of 20% (w/v) acetic acid (pH 3.5), 1500 μl of 0.8% (w/v) thiobarbituric acid and 700 μl distilled water.

Samples were then boiled for 1 h at 95°C and centrifuged at 3000xg for 10 min. The absorbance of the supernatant was measured by spectrophotometry at 515–553 nm.

*Immunohistochemical localization of GFAP, nitrotyrosine, PAR , FasL, Bax and Bcl-2, S-100*

At 24 h after SCI, the tissues were fixed in 10% (w/v) PBS-buffered formaldehyde and 8 μm sections were prepared from paraffin embedded tissues. After deparaffinization, endogenous peroxidase was quenched with 0.3% (v/v) hydrogen peroxide in 60% (v/v) methanol for 30 min. The sections were permeablized with 0.1% (w/v) Triton X-100 in PBS for 20 min. Non-specific adsorption was minimized by incubating the section in 2% (v/v) normal goat serum in PBS for 20 min. Endogenous biotin or avidin binding sites were blocked by sequential incubation for 15 min with biotin and avidin, respectively. Sections were incubated overnight with anti-nitrotyrosine rabbit polyclonal antibody (Upstate, 1:500 in PBS, v/v; Upstate, Millipore, Milan, Italy), anti-PAR antibody (BioMol, 1:200 in PBS, v/v; BioMol, Milan, Italy), anti-FasL antibody (Santa Cruz Biotechnology, Santa Cruz, CA, 1:500 in PBS, v/v), anti-Bax antibody (Santa Cruz Biotechnology, 1:500 in PBS, v/v), anti-Bcl-2 polyclonal antibody (Santa Cruz Biotechnology, 1:500 in PBS, v/v), anti-S100 polyclonal antibody (Santa Cruz Biotechnology, 1:500 in PBS, v/v) or with anti-GFAP polyclonal antibody (Santa Cruz Biotechnology, 1:500 in PBS, v/v). Sections were washed with PBS and incubated with secondary antibody. Specific labelling was detected with a biotin-conjugated goat anti-rabbit IgG and avidin-biotin peroxidase complex (Vector Laboratories, DBA, Milan, Italy). To verify the binding specificity for nitrotyrosine, PAR, FasL, S-100, Bax and Bcl-2, GFAP, some sections were also incubated with only the primary antibody (no secondary) or with only the secondary antibody (no primary). In these situations no positive staining was found in the sections indicating that the immunoreactions were positive in all the experiments carried out. Immunocytochemistry photographs ($n=5$ photos from each samples collected from all mice in each experimental group) were assessed by densitometry using Optilab Graftek software (Milan, Italy) on a Macintosh personal computer.

*Western blot analysis for IκB-α, NF-κB p65, Bax, Bcl-2 and iNOS*

Cytosolic and nuclear extracts were prepared as previously described [15] with slight modifications. Briefly, spinal cord tissues from each mouse were suspended in extraction Buffer A containing 0.2 mM phenylmethylsulphonyl fluoride (PMSF), 0.15 μM pepstatin A, 20 μM leupeptin, 1 mM sodium orthovanadate, homogenized at the highest setting for 2 min and centrifuged at 1000 x g for 10 min at 4°C. Supernatants represented the cytosolic fraction. The pellets, containing enriched nuclei, were re-suspended in Buffer B containing 1% Triton X-100, 150 mM NaCl, 10 mM TRIS-HCl pH 7.4, 1 mM ethylene glycol-bis(beta-aminoethyl ether)-N,N,N',N'-tetraacetic acid (EGTA), 1 mM ethylene diamine-tetra-acetic acid (EDTA), 0.2 mM PMSF, 20 μM leupeptin and 0.2 mM sodium orthovanadate. After centrifugation for 30 min at 15 000 × g at 4°C, the supernatants containing the nuclear protein were stored at -80°C for further analysis. The levels of IκB-α, iNOS, Bax and Bcl-2 were quantified in cytosolic fractions from spinal cord tissue collected 24 h after SCI, while NF-κB p65 levels were quantified in nuclear fractions. The filters were blocked with 1× PBS, 5% (w/v) non-fat dried milk (PM) for 40 min at room temperature and subsequently probed with specific Abs IκB-α (1:1000 Santa Cruz Biotechnology; DBA, Milan, Italy) or phospho-NF-κB p65 (serine 536) (1:1000, Cell Signaling; DBA, Milan, Italy), anti-Bax (1:500; Santa Cruz Biotechnology; DBA, Milan, Italy), anti-Bcl-2

(1:500; Santa Cruz Biotechnology; DBA, Milan, Italy), anti-iNOS, (1:1000 Signal Trasduction) or anti-NF-κB p65 (1:1000; Santa Cruz Biotechnology) in 1x PBS, 5 % w/v non-fat dried milk, 0.1% Tween-20 (PMT) at 4°C, overnight. Membranes were incubated with peroxidase-conjugated bovine anti-mouse IgG secondary antibody or peroxidase-conjugated goat anti-rabbit IgG (1:2000, Jackson ImmunoResearch, West Grove, PA) for 1 h at room temperature.

To ascertain that blots were loaded with equal amounts of proteic lysates, they were also incubated in the presence of the antibody against β-actin (1:10 000 Sigma-Aldrich Corp; Milan, Italy) and laminin B-1 (1:5,000, Sigma Aldrich Corp). The relative expression of the protein bands of IκB-α (~ 37 kDa), iNOS (~ 130 kDa), NF-κB p65 (65 kDa), Bax (~ 23 kDa) and Bcl-2 (~ 29 kDa) was quantified by densitometric scanning of the X-ray films with GS-700 Imaging Densitometer (GS-700, Bio-Rad Laboratories, Milan, Italy) and a computer program (Molecular Analyst, IBM).

### *Terminal deoxynucleotidyltransferase-mediated UTP end labelling (TUNEL) assay*

TUNEL assay was conducted by using a TUNEL detection kit according to the manufacturer's instruction (Apotag, HRP kit DBA, Milan, Italy). Briefly, tissue segments containing the lesion (1 cm on each side of the lesion, rostrally/caudally to the perilesional area) were cut into longitudinal 5-μm-thick sections. Tissue were incubated with 15 μg/ml proteinase K for 15 min at room temperature and then washed with PBS. Endogenous peroxidase was inactivated by 3% $H_2O_2$ for 5 min at room temperature and then washed with PBS. Sections were immersed in terminal deoxynucleotidyltransferase (TdT) buffer containing deoxynucleotidyl transferase and biotinylated dUTP in TdT buffer, incubated in a humid atmosphere at 37°C for 90 min and then washed with PBS. The sections were incubated at room temperature for 30 min with anti-horseradish peroxidase-conjugated antibody and the signals were visualized with diaminobenzidine. The number of TUNEL positive cells/high-power field was counted in five-to-10 fields for each coded slide.

### *Grading of motor disturbance*

The motor function of mice subjected to compression trauma was assessed once a day for 10 days after injury. Recovery from motor disturbance was graded using the modified murine Basso, Beattie, and Bresnahan (BBB) [16] hind limb locomotor rating scale [17,18].

### *Materials*

The primary antibodies directed at FasL, Bax and Bcl-2 was obtained from Santa Cruz Biotechnology, Inc.. The secondary antibody was obtained from Jackson Immuno Research, Laboratories, Inc. Unless otherwise stated, all compounds were obtained from Sigma-Aldrich Company Ltd. (Milan, Italy). All other chemicals were of the highest commercial grade available. All stock solutions were prepared in non-pyrogenic saline (0.9% NaCl; Baxter, Italy, UK).

### *Statistical evaluation*

All values in the figures and text are expressed as mean ± standard error of the mean (SEM) of *n* observations. For the *in vivo* studies *n* represents the number of animals studied. In the experiments involving histology or immunohistochemistry, the figures shown are representative of at least three experiments performed on different experimental days. The results were analysed by one-way ANOVA followed by a Bonferroni *post-hoc* test for multiple comparisons. A $p$-value of less than 0.05 was considered significant. BBB scale data were analysed by the Mann-Whitney test and considered significant when $p$-value was $< 0.05$.

## Results

### *Effects of DFO on the severity of spinal cord trauma*

The severity of the trauma at the level of the perilesional area, assessed by the presence of oedema as well as alteration of the white matter and infiltration of leukocytes (Figure 1B, see histological score D), was evaluated at 24 h after injury. Significant damage to the spinal cord was observed in the spinal cord tissue from SCI mice when compared with sham-operated mice (Figure 1A, see histological score D). Notably, significant protection against the SCI was observed in DFO -treated mice (Figure 1C, see histological score D). Reticular and nervous fibres tissue structures were observed by silver impregnation. In sham-treated mice a normal presence of reticular and nervous fibres was observed (Figure 1E). On the contrary a significant alteration of reticular and nervous fibres was observed in the spinal cord tissues collected at 24 h after SCI (Figure 1F). DFO treatment significantly reduced the alteration of reticular and nervous fibres associated with SCI (Figure 1G).

In order to evaluate if histological damage to the spinal cord was associated with a loss of motor function, the modified BBB hind limb locomotor rating scale score was evaluated. While motor function was only slightly impaired in sham mice, mice subjected to SCI had significant deficits in hind limb movement (Figure 1H). DFO reduced the ameliorated functional deficits induced by SCI (Figure 1H).

### *Effects of DFO on the severity of astrocytic reaction to SCI*

GFAP immunohistochemistry in the sham groups revealed astrocytic cell bodies evenly dispersed

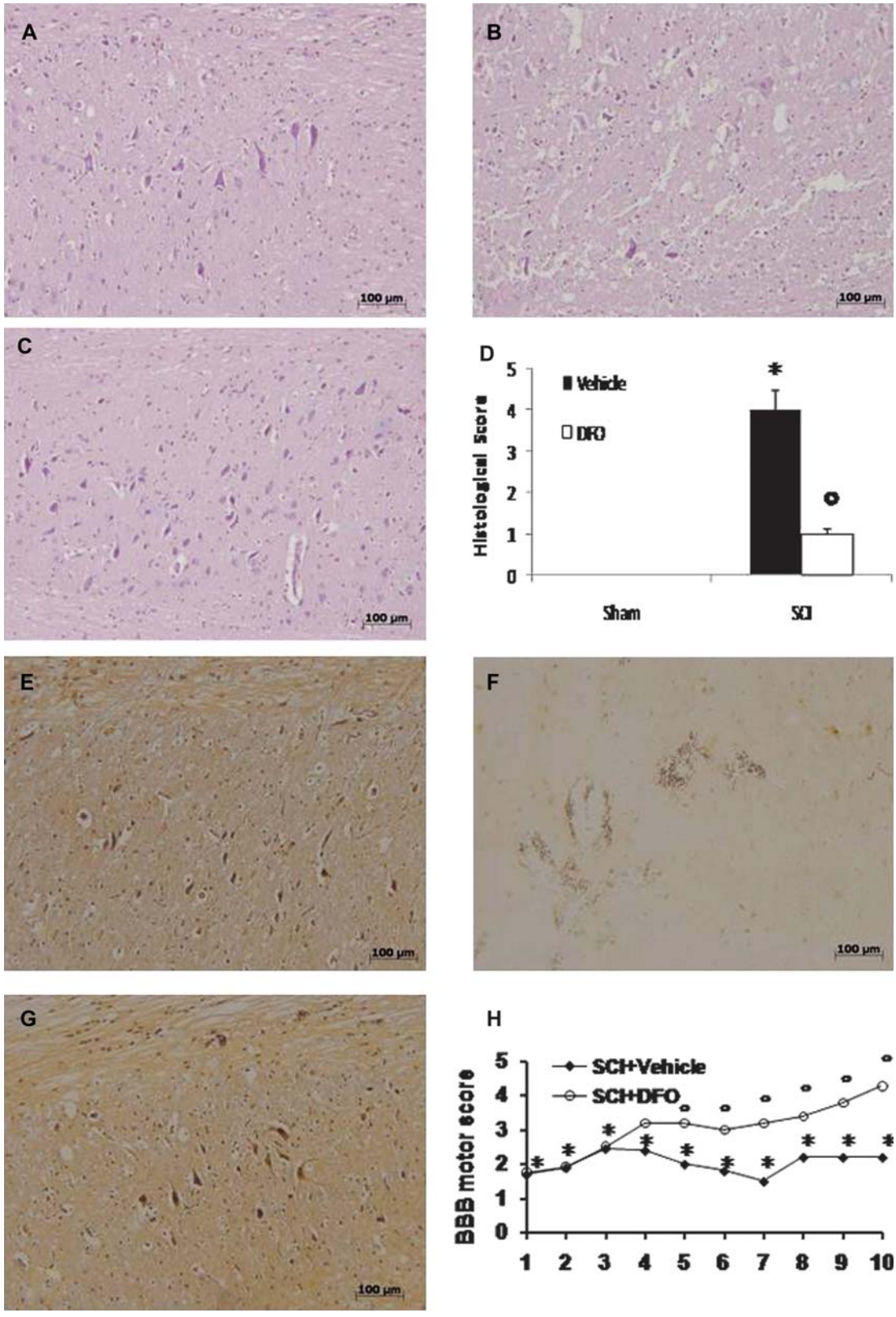


Figure 1. Effect of DFO treatment on histological alterations of the spinal cord tissue 24 h after injury and motor function. Significant damage to the spinal cord in mice subjected to SCI, at the perilesional area, was apparent, as evidenced by the presence of oedema as well as alteration of the white matter 24 h after injury (B). Notably, a significant protection from SCI-associated damage was observed in the tissue samples collected from DFO treated mice (C). No significant damage was observed in the spinal cord tissue from sham-operated mice (A). The histological score (D) was made by an independent observer. In sham-treated mice a normal presence of reticular and nervous fibres was observed (E). On the contrary in the spinal cord tissues collected at 24 h after SCI (F), was observed a significant alteration of reticular and nervous fibres. DFO treatment significantly reduced the alteration of reticular and nervous fibres associated with SCI (G). The degree of motor disturbance was assessed every day until 10 days after SCI by Basso, Beattie, and Bresnahan criteria (H). Treatments with DFO enhanced the recovery after SCI. This figure is representative of at least three experiments performed on different experimental days. Data are means ± SE of 10 mice for each group. $^{*}p < 0.01$ vs Sham. $^{\circ}p < 0.01$ vs SCI + vehicle.

throughout spinal cord gray and white matter, scattered between the networks of astrocytic processes (data not shown). At 24 h after trauma, the sections of spinal cord obtained by SCI+vehicle group mice showed perilesional, highly GFAP-positive, activated astrocytes. These cells were distributed homogeneously over white and gray matter in particles proximal and distal to the lesion site (Figure 2A). Spinal cord tissue by mice with DFO treatment, instead demonstrated a massive reduction of GFAP immunoreactivity (Figure 2B).

*Effects of DFO on neutrophil infiltration after SCI*

The above-mentioned histological pattern of spinal cord injury appeared to be correlated with the influx of leukocytes into the spinal cord. Therefore, we investigated the effect of DFO on neutrophil infiltration by measuring tissue MPO activity. MPO activity was significantly elevated in the spinal cord at 24 h after injury in mice subjected to SCI when compared with sham-operated mice (Figure 3). Treatment with DFO attenuated neutrophil infiltration into the spinal cord at 24 h after injury (Figure 3).

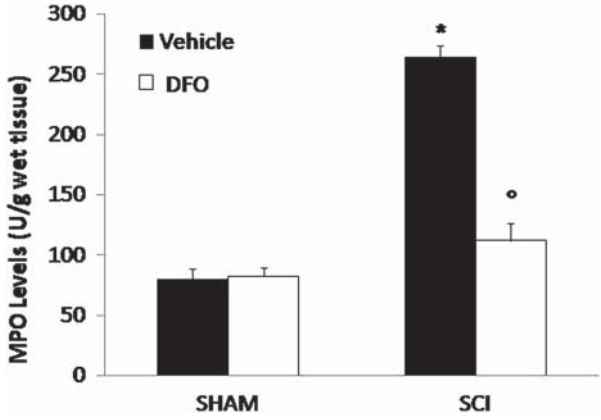


Figure 3. Effects of DFO on MPO activity. Following the injury, MPO activity in spinal cord from SCI mice was significantly increased at 24 h after the damage in comparison to sham mice. Treatment with DFO attenuated neutrophil infiltration into the spinal cord in a dose-dependent fashion. Data are means ± SE of 10 mice for each group. $^{*}p < 0.01$ vs Sham. $^{\circ}p < 0.01$ vs SCI+vehicle.

*Effect of DFO on IκB-α degradation and NF-κB p65 activation after SCI*

We evaluated IκB-α degradation and nuclear NF-κB p65 expression by Western blot analysis to investigate the cellular mechanisms whereby treatment with DFO attenuates the development of SCI. Basal expression of IκB-α was detected in spinal cord samples from sham-operated animals, whereas IκB-α levels were substantially reduced in SCI mice (Figures 4A and A1). DFO treatment prevented SCI-induced IκB-α degradation (Figures 4A and A1). In addition, NF-κB p65 levels in the spinal cord nuclear fractions were also significantly increased at 24 h after SCI compared to the sham-operated mice (Figures 4B and B1). DFO treatment significantly reduced the levels of NF-κB p65, as shown in Figures 4B and B1.

*Effects of DFO on modulation of iNOS expression after SCI*

To determine the role of nitric oxide (NO) produced during SCI, iNOS expression was evaluated by Western blot. A significant increase of iNOS (Figures 5A and A1) levels were observed in the spinal cord from mice subjected to SCI. On the contrary, DFO treatment prevented the SCI-induced iNOS expression (Figures 5A and A1).

*Effects of DFO on nitrotyrosine formation and lipid peroxidation, after SCI*

Twenty-four hours after SCI, nitrotyrosine, a specific marker of nitrosative stress, was measured by immunohistochemical analysis in the spinal cord sections to determine the localization of various reactive nitrogen species produced during SCI. Spinal cord sections from

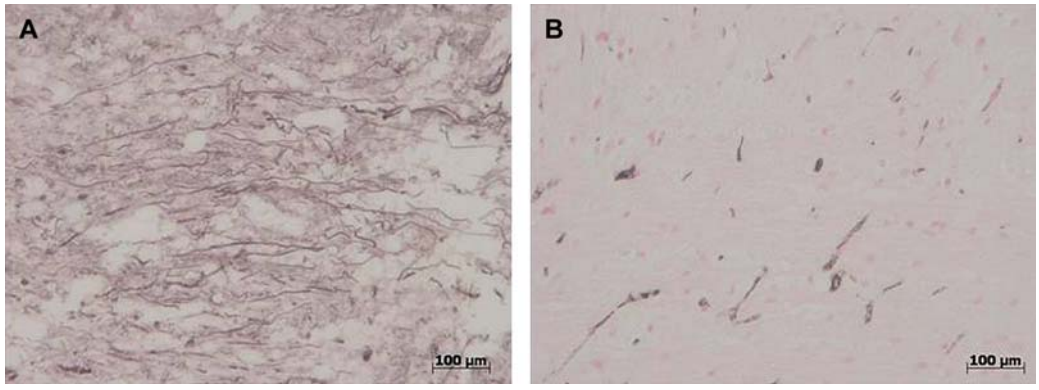


Figure 2. Effects of DFO on astrocytic reaction. Tissue sections obtained from vehicle-treated animals after SCI demonstrate positive staining for GFAP mainly localized in perilesional activated astrocytes (A). DFO treatment reduced the degree of positive staining for GFAP (B) in the spinal cord. The assay was carried out by using Optilab Graftek software on a Macintosh personal computer (CPU G3-266).

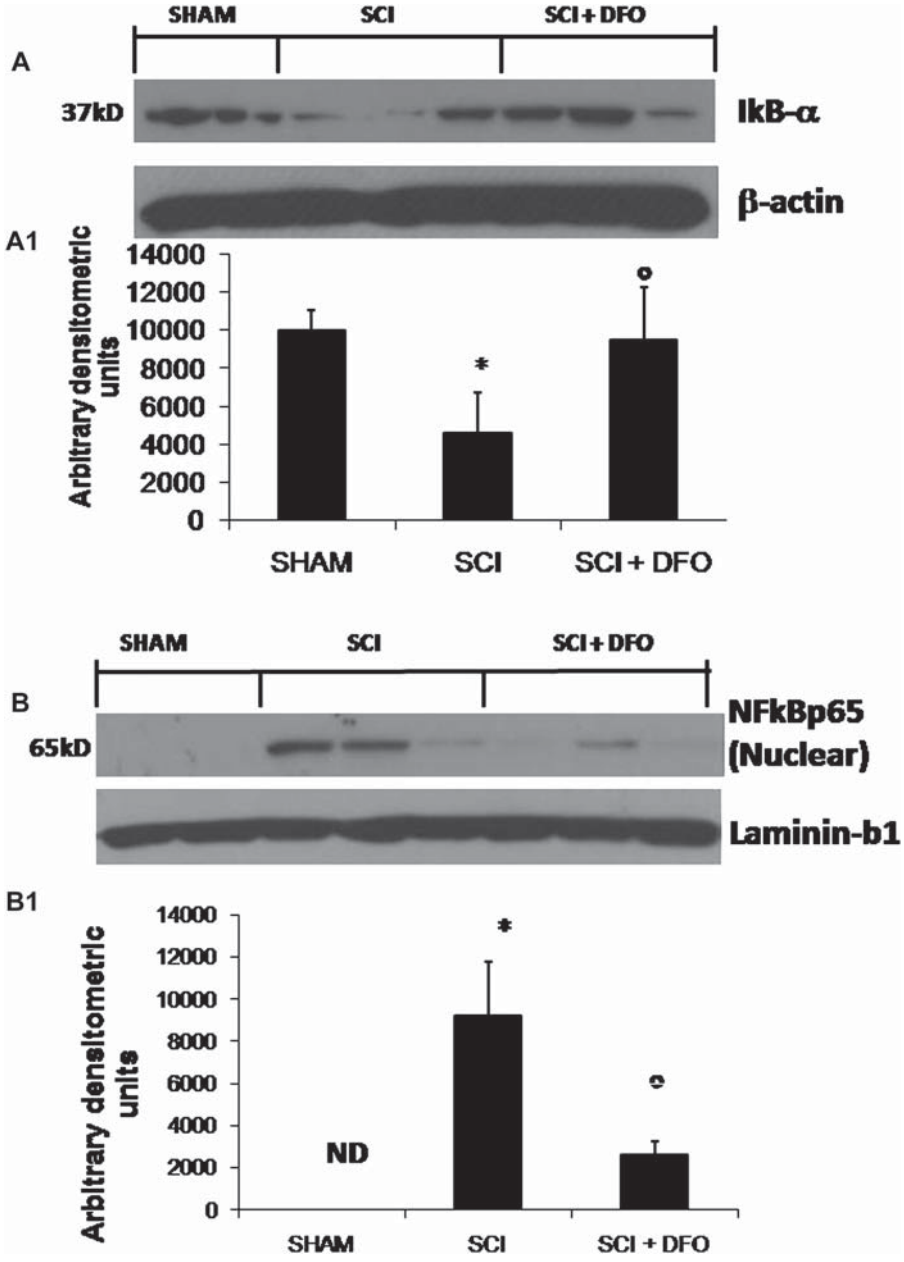


Figure 4. Effects of DFO treatment on IκB-α degradation, phosphorylation and total NF-κB p65. By Western Blot analysis, a basal level of IκB-α was detected in the spinal cord from sham-operated animals, whereas in SCI mice IκB-α levels were substantially reduced. DFO treatment prevented the SCI-induced IκB-α degradation (A, $A_1$). In addition, SCI caused a significant increase in nuclear NF-κB p65 compared to the sham-operated mice (B, $B_1$). DFO treatment significantly reduced the NF-κB p65 levels (B, $B_1$). Immunoblotting in (A) and (B) is representative of one spinal cord tissues out of 5–6 analysed. The results in ($A_1$) and ($B_1$) are expressed as mean ± SEM from 5–6 spinal cord tissues. $^{*}p < 0.01$ vs Sham; $^{\circ}p < 0.01$ vs SCI.

sham-operated mice did not stain for nitrotyrosine (data not shown), whereas spinal cord sections obtained from SCI mice exhibited positive staining for nitrotyrosine (Figure 6A, see densitometry analysis C). The positive staining was mainly localized in inflammatory cells as well as in nuclei of Schwann cells in the white and gray matter of the spinal cord tissues. DFO reduced the degree of positive staining for nitrotyrosine (Figure 6B, see densitometry analysis C) in the spinal cord. In addition, at 24 h after SCI, levels of MDA were also measured in the spinal cord tissue as an indicator of lipid peroxidation. As shown in Figure 6D, MDA levels were present at significantly higher levels in spinal cord tissue collected from mice subjected to SCI when compared with sham-operated mice. Lipid peroxidation was significantly attenuated by treatment with DFO (Figure 6D).

### *Effects of DFO on DNA/RNA alteration and PAR formation in spinal cord after injury*

The simultaneous presence of DNA and RNA was detected by methyl green pyronin staining. In sham animals (Figure 7A), the simultaneous presence of

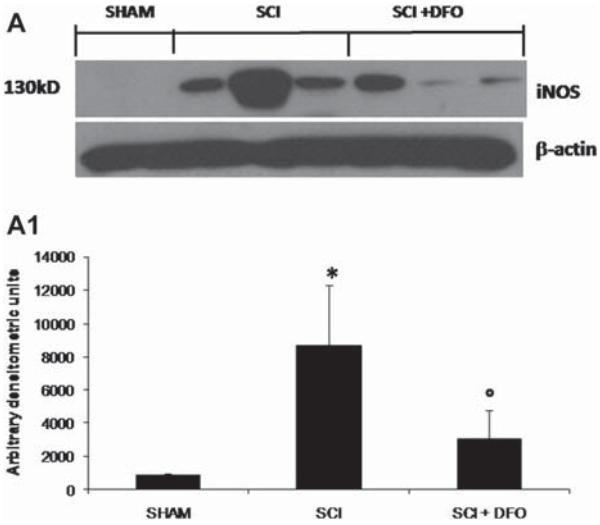


Figure 5. Effects of DFO on iNOS expression in spinal cord tissue. iNOS levels by Western blot analysis were significantly increased in the spinal cord from SCI mice (A). On the contrary, DFO treatment significantly reduced the SCI-induced expression of iNOS (A). The relative expression of the protein band was standardized for densitometric analysis to β-actin levels (A1) and expressed as mean ± SEM from $n = 5/6$ spinal cord for each group. $^{*}p < 0.01$ vs Sham. $^{\circ}p < 0.01$ vs SCI + vehicle.

DNA and RNA clearly stained by methyl green pyronin staining in both lateral and dorsal funiculi of the spinal cord. At 24 h after the injury, a significant loss of DNA and RNA presence in lateral and dorsal funiculi was observed in control mice subjected to SCI (Figure 7B). In contrast, in DFO-treated mice, the DNA and RNA degradation was attenuated in the central part of lateral and dorsal funiculi (Figure 7C). In addition, in our study, immunohistochemistry for PAR, as an indicator of *in vivo* PARP activation, revealed the occurrence of positive staining for PAR localized in nuclei of Schwann cells in the white and gray matter of the spinal cord tissues from mice subjected to SCI (Figure 7D, see densitometry analysis F). DFO treatment reduced the degree of positive staining for PAR (Figure 7E, see densitometry analysis F) in the spinal cord.

### *Effects of DFO on expression of FasL after SCI*

Immunohistological staining for FasL in the spinal cord was also determined 24 h after injury. Spinal cord sections from sham-operated mice did not stain for FasL (data not shown), whereas spinal cord sections obtained from SCI mice exhibited positive staining for FasL (Figure 8A, and see densitometry analysis C) mainly localized in various cells in the gray matter (Figure 8A) . DFO reduced the degree of positive staining for FasL in the spinal cord (Figure 8B and see densitometry analysis C).

### *Effects of DFO on apoptosis in spinal cord after injury*

To test whether the tissue damage was associated with the induction of apoptosis, we evaluated TUNEL-like staining in the perilesional spinal cord tissue at 24 h after injury. No apoptotic cells were detected in the spinal cord from sham-operated mice (data not shown). At 24 h after the trauma, tissues from SCI mice demonstrated a marked appearance of dark brown apoptotic cells and intercellular apoptotic fragments (Figure 9A). In contrast, tissues obtained from mice treated with DFO demonstrated no apoptotic cells or fragments (Figure 9B).

### *Effects of DFO on expression of Bax and Bcl-2 after injury*

The appearance of Bax in homogenates of spinal cord was investigated by Western blot at 24 h after SCI. A basal level of Bax was detected in the spinal cord from sham-operated animals (Figures 10A and A1). Bax levels were substantially increased in the spinal cord from saline-treated mice subjected to SCI (Figures 10A and A1). The treatment with DFO decreased the SCI-induced Bax expression (Figures 10A and A1).

To detect Bcl-2 expression, whole extracts from spinal cord of each mouse were also analysed by Western blot analysis. A low basal level of Bcl-2 expression was detected in spinal cord from sham-operated mice (Figures 10B and $B_1$). Twenty-four hours after SCI, the Bcl-2 expression was significantly reduced in whole extracts obtained from spinal cord of SCI + saline mice group (Figures 10B and $B_1$). Treatment with DFO decreased significantly the SCI-induced inhibition of Bcl-2 expression (Figures 10B and $B_1$).

Moreover, samples of spinal cord tissue were taken at 24 h after SCI also to determine the immunohistological staining for Bax and Bcl-2. Spinal cord sections from sham-operated mice did not stain for Bax (data not shown), whereas spinal cord sections obtained from SCI mice exhibited a positive staining for Bax (Figure 10C, and see densitometry analysis G). DFO reduced the degree of positive staining for Bax in the spinal cord of mice subjected to SCI (Figure 10D, and see densitometry analysis G). In addition, spinal cord sections from sham-operated mice demonstrated Bcl-2 positive staining (data not shown) while in SCI mice the staining significantly reduced (Figure 10D, and see densitometry analysis G). DFO attenuated the loss of positive staining for Bcl-2 in the spinal cord from SCI- subjected mice (Figure 10E, and see densitometry analysis G).

### *Effects of DFO S100β immunoreactivity after injury*

S100β immunoreactive quiescent astrocytes with a small size and thin processes were seen distributed throughout the white and gray matters of the studied levels of the sham-operated mice (data not shown). The SCI in the saline mice group increased the number of S100β immunoreactive astrocytes with a large cytoplasm and thick processes, in the white and gray

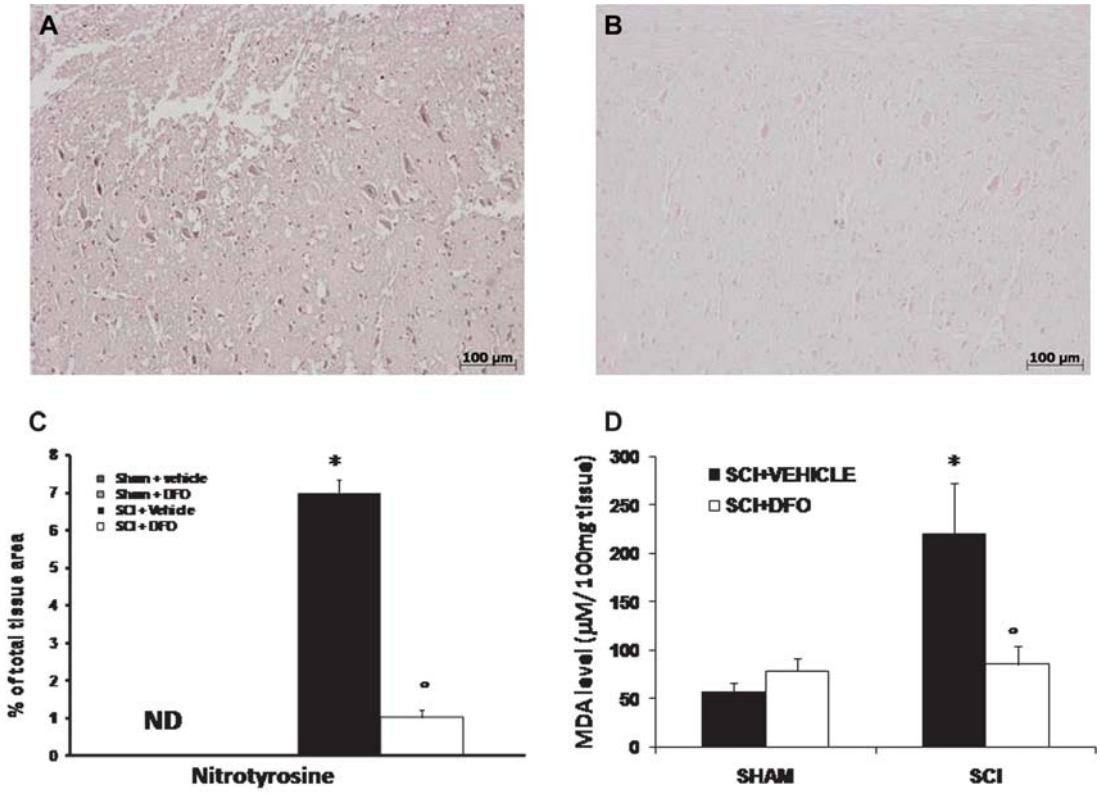


Figure 6. Effects of DFO on nitrotyrosine formation and lipid peroxidation. Tissue sections obtained from vehicle-treated animals after SCI demonstrate positive staining for nitrotyrosine mainly localized in inflammatory, in nuclei of Schwann cells in the white and gray matter (A). DFO treatment reduced the degree of positive staining for nitrotyrosine (B) in the spinal cord. Densitometry analysis of immunocytochemistry photographs ($n=5$ photos from each sample collected from all mice in each experimental group) for nitrotyrosine (C) from spinal cord tissues was assessed. In addition, MDA levels in the spinal cord from SCI mice (D) were significantly increased in SCI operated mice in comparison to sham. DFO-treated mice show a significant reduction of MDA levels (D). Values are mean ± SEM of 10 rats for each group. The assay was carried out by using Optilab Graftek software on a Macintosh personal computer (CPU G3-266). Data are expressed as a percentage of total tissue area. This figure is representative of at least three experiments performed on different experimental days. Data are means ± SE of 10 mice for each group. $^{*}p < 0.01$ vs Sham. $^{\circ}p < 0.01$ vs SCI + vehicle.

matters of the spinal cord at cranial and caudal levels adjacent to the injury (Figure 11A, see densitometric analysis C). This number of S100β immunoreactive astrocytes is decreased in the spinal cord obtained from SCI + DFO-treated mice (Figure 11B, see densitometric analysis C).

## Discussion

The condition often occurs following spinal cord injury and causes greater damage after SCI, is the subsequent secondary neurodegeneration that takes place in the surrounding injured tissue. Even so, today, there is not enough information regarding the cellular and molecular mechanisms which occur and govern the inflammation after SCI; excessive inflammation damages surrounding healthy tissue. In fact, microglia releases pro-inflammatory and cytotoxic factors, nitric oxide (NO), reactive oxygen species (ROS), etc. Much of the damage that occurs in the spinal cord following traumatic injury is due to the secondary effects of glutamate excitotoxicity, $Ca^{2+}$ overload and free iron [6], mechanisms that take part in a spiralling interactive cascade ending in neuronal dysfunction and death. In these conditions several therapies targeting various factors involved in the secondary degeneration cascade lead to tissue sparing and improved behavioural outcomes in spinal cord-injured animals. Several authors have demonstrated that free iron can cause free radical formation and oxidative brain damage [19]. Iron is known to potentiate the toxic effects of ROS by catalysing the formation of highly reactive hydroxyl radicals from hydrogen peroxide through the so-called Fenton chemistry. Thus, while iron is essential for normal physiology [20], it is also implicated in many pathological processes, including neuron degenerative disorders [21]. DFO has been widely used clinically for removal of excess iron from the body, such as in acute iron poisoning and haemochromatosis [7]. Moreover, data presents by Yu et al. [7] suggest that DFO may also be useful for protection against motor neuron degeneration by measuring its protective activity of iron chelating. These results are in agreement with our study, which shows that DFO ameliorates lesion in the spinal cord after injury, suggesting that it reduced iron-mediated oxidative DNA damage. These and other results were reported in the literature [19,22] and indicate that iron may contribute to oxidative spinal cord

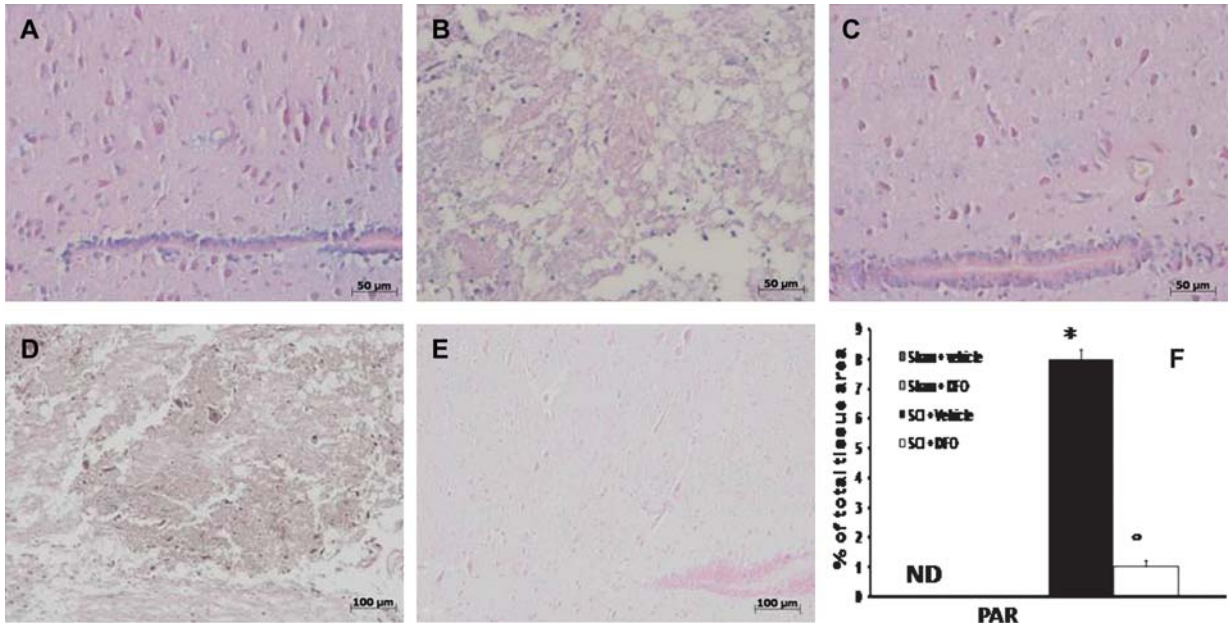


Figure 7. Effects of DFO on the presence of DNA and RNA (assessed by methyl green pyronin staining). In sham animals, the simultaneous presence of DNA and RNA was clearly evidenced by methyl green pyronin staining in both lateral and dorsal funiculi of the spinal cord (A). At 24 h after the injury, a significant loss of DNA and RNA presence was observed in SCI mice (B). In contrast, the DNA and RNA degradation was attenuated in the central part of lateral and dorsal funiculi after DFO treatment (C). In addition, immunohistochemistry for PAR, an indicator of *in vivo* PARP activation, revealed the occurrence of positive staining for PAR localized in nuclei of Schwann cells in wm and gm of the spinal cord tissues from SCI mice (D). DFO treatment reduced the degree of positive staining for PAR (E) in the spinal cord. Densitometry analysis of immunocytochemistry photographs ($n=5$ photos from each sample collected from all mice in each experimental group) for PAR (F) from spinal cord tissues was assessed. The assay was carried out by using Optilab Graftek software on a Macintosh personal computer (CPU G3-266). Data are expressed as a percentage of total tissue area. This figure is representative of at least three experiments performed on different experimental days. Data are means ± SE of 10 mice for each group. $^{*}p < 0.01$ vs Sham. $^{\circ}p < 0.01$ vs SCI + vehicle.

damage after trauma and that iron is a target in SCI treatment. In this regard, it has been demonstrated that DFO can penetrate the blood–brain barrier and accumulate in the brain tissue at a significant concentration quickly after subcutaneous injection [23,24]. The initial half-life of DFO after intravenous infusion is 0.28 h and the terminal half-life is 3.05 h [25].

In this report we demonstrate that DFO exerts beneficial effects in a mice model of spinal cord injury. Since it has been demonstrated that SCI leads to tissue oedema and loss of myelin in lateral and dorsal funiculi and that this histological pattern is associated to the loss of motor function, here we demonstrated that treatment with DFO exerts an evident protection, ameliorating the morphology of tissue as demonstrated by H&E, silver impregnation and as well as preventing activation of astrocytes as indicated by decreases in the atrocity reactive marker GFAP.

GFAP is an intermediate filament that is expressed at highest levels in astrocytes of the CNS, but is also found in several other isolated cell types such as enteric glia and non-myelinating Schwann cells [26].

In a very short time after traumatic SCI, ischemia, oxidative damage, oedema and glutamate excitotoxicity all contribute to substantial secondary damage events. The infiltration of inflammatory cells that immediately follow trauma then may play a major role in expansion of the lesion size. We found a correlation between the areas of necrosis and presence of inflammatory cells which often extended into tissue adjacent to the lesion centre. In agreement with previous studies [27], we have observed in this experimental setting that the infiltration of neutrophils at the injury site 24 h following SCI is significantly increased in all animals. Treatment with DFO markedly reduced the neutrophils infiltration, suggesting that iron chelation therapy and the antioxidant effects of DFO may play an important role in the regulation of inflammatory cells infiltration.

Another potential mechanism by which DFO could improve secondary damage in our experimental model of SCI is by regulating the activation of NF-κB that occurs at the transcriptional level.

It's a known fact that one consequence of increased oxidative stress is the activation and inactivation of redox-sensitive proteins like NF-κB. NF-κB is normally sequestered in the cytoplasm, bound to regulatory proteins IκBs. In response to a wide range of stimuli including oxidative stress, infection, hypoxia, extracellular signals and inflammation, IκB is phosphorylated by the enzyme IκB kinase. The net result is the release of the NF-κB dimer, which is then free to translocate into the nucleus.

In this study we also demonstrate that the DFO inhibiting the IκB-α degradation prevent NF-κB translocation into the nucleus and subsequent activation of many pro-inflammatory genes. In fact NF-κB

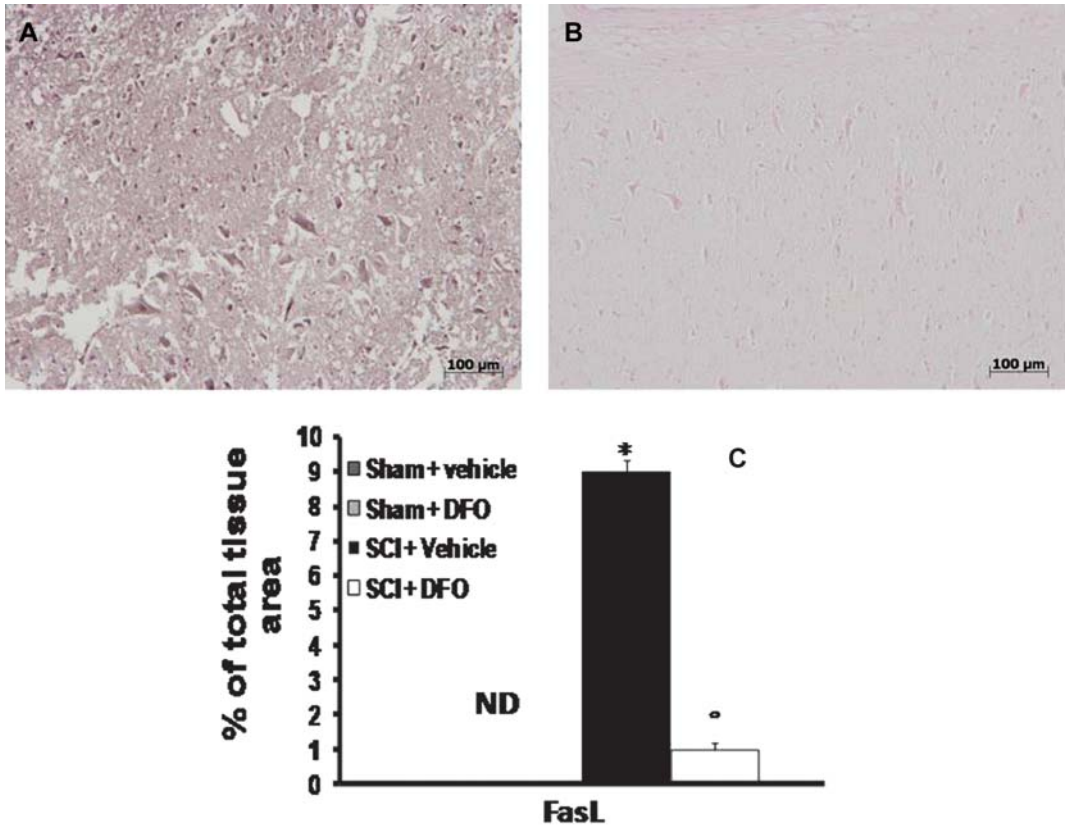


Figure 8. Effect of DFO on immunohistochemical localization and expression of FasL. Spinal cord sections were processed at 24 h after SCI to determine the immunohistological staining for FasL. A substantial increase in FasL (A) expression was found in inflammatory cells, in nuclei of Schwann cells in the spinal cord tissues from SCI mice. Spinal cord levels of FasL (B) were significantly attenuated in DFO-SCI treated mice in comparison to SCI animals. Densitometry analysis of immunocytochemistry photographs ($n=5$ photos from each sample collected from all mice in each experimental group) for FasL (C) from spinal cord tissues was assessed. The assay was carried out by using Optilab Graftek software on a Macintosh personal computer (CPU G3-266). This figure is representative of at least three experiments performed on different experimental days. $^{*}p < 0.01$ vs Sham. $^{\circ}p < 0.01$ vs SCI+vehicle.

plays a central role in the regulation of many genes responsible for the generation of mediators or proteins in inflammation, these include the genes for TNF-α, IL-1β, iNOS and COX-2, to name but a few.

In this study we demonstrate that DFO attenuates the expression of iNOS in the tissue from SCI-treated mice when compared with untreated injured mice. It has been reported that NO directly controls intracellular iron metabolism by activating iron regulatory protein (IRP), a cytoplasmic protein that control ferritin translation [28]. Other authors investigated the neurotoxic role of NO after intracerebroventricular injection of iron on the cerebellar Purkinje cells in the rat, showing that inhibition of the neuronal NOS prevented some of the deleterious effects of iron on cerebellar Purkinje cells [29].

It has also been demonstrated that enhanced formation of NO by iNOS contributes to SCI. In the present study we clearly demonstrate that DFO treatment fully inhibited the appearance of nitrotyrosine staining in the inflamed tissue. This effect is likely related to a well-known antioxidant property of DFO on peroxynitrite, as demonstrated by other authors [30].

The antioxidant activities of DFO were also assessed in an *in vitro* system, reducing protein nitration, restoring enzyme activities and maintaining erythrocyte membrane integrity.

Nitrotyrosine formation was initially proposed as a relatively specific marker for the detection of the endogenous formation 'footprint' of peroxynitrite. There is, however, recent evidence that other reactions can also induce tyrosine nitration; e.g. the reaction of nitrite with hypochlorous acid and the reaction of myeloperoxidase with hydrogen peroxide can lead to the formation of nitrotyrosine [31]. Increased nitrotyrosine staining is considered, therefore, as an indication of 'increased nitrosative stress' rather than a specific marker of the peroxynitrite generation.

Malondialdehyde (MDA) levels, as an indicator of lipid peroxidation, were determined in the spinal cord tissue at 24 h after SCI. In this study, in agreement with previous reports [32], we demonstrated that DFO treatment reduced MDA levels injured tissue. In fact, it's known that DFO is able to improve injury by chelating iron, thereby inhibiting lipid peroxidation and free radical formation.

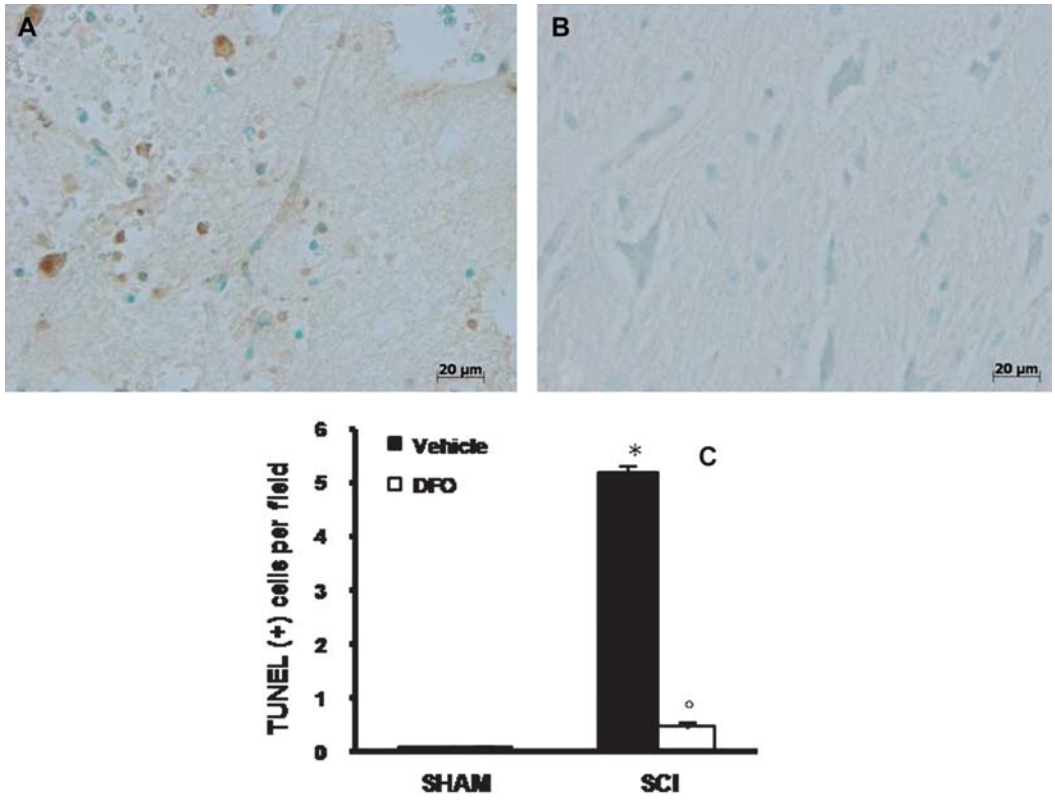


Figure 9. Effects of DFO on TUNEL-like staining in the perilesional spinal cord tissue. At 24 h after the trauma, SCI mice demonstrated a marked appearance of dark brown apoptotic cells and intercellular apoptotic fragments (A). In contrast, tissues obtained from mice treated with DFO had no apoptotic cells or fragments (B). The number of TUNEL positive cells/high-power field was counted in five-to-10 fields for each coded slide (C). Figure is representative of at least three experiments performed on different experimental days.

The postulated pathophysiological mechanisms suggest that iron-catalysed lipid peroxidation plays an important role in the auto-destruction of the injured spinal cord [33].

ROS and peroxynitrite also cause DNA damage, which results in the alteration of mitochondrial respiration as well as activation of the nuclear enzyme poly(ADP-ribose) polymerase (PARP), depletion of $NAD^+$ and ATP and ultimately cell death [34]. This pathway plays an important role in various forms of inflammation and neurodegenerative disease. It is conceivable that by scavenging hydroxyl radical and peroxynitrite, DFO would prevent the DNA single strand breakage and thus prevent the activation of PARS in inflammation. We demonstrate here that DFO reduced the increase in PARP activation in the spinal cord from SCI-operated mice. Thus, we propose that the anti-inflammatory effects of DFO may be due to the prevention of the activation of PARP. These data are in agreement with other authors that demonstrated DFO reduced haemoglobin-induced brain oedema and activation of PARP [35] . To further confirm the data about the prevention of damage to DNA, we have used Methyl-green-pyronin staining, a differential nucleic acid staining, which distinguishes the double and single stranded states of the nucleic acids and we obtained that DFO prevented the alteration of nucleic acid.

Lesions and trauma to the brain of spinal cord cause an inflammatory response of the white matter tracts resulting in wallerian degeneration of the distal axonal segment, which has been separated from its parent cell body [36]. Wallerian degeneration may be associated with apoptosis after injuries in the CNS. Iron chelators can induce both cell cycle arrest and programmed cell death or apoptosis.

Apoptosis is an important mediator of secondary damage after SCI. It incurs its affects through at least two phases: an initial phase, in which apoptosis accompanies necrosis in the degeneration of multiple cell types, and a later phase, which is predominantly confined to white matter and involves oligodendrocytes and microglia. In an effort to prevent or diminish levels of apoptosis, we have demonstrated that the treatment with DFO attenuates the degree of apoptosis, measured by TUNEL detection kit, in the spinal cord after the damage.

Thus, iron chelation has been shown to induce apoptosis in Kaposi's sarcoma cells [37] and neuroblastoma cells. The human leukaemic cell line CCRF-CEM treated with DFO exhibited morphological features of apoptosis after 48 h.

Mechanisms of apoptosis mediated by iron chelators are poorly understood. The data obtained here were realized to determine the molecular pathway utilized by iron chelators to prevent apoptosis.

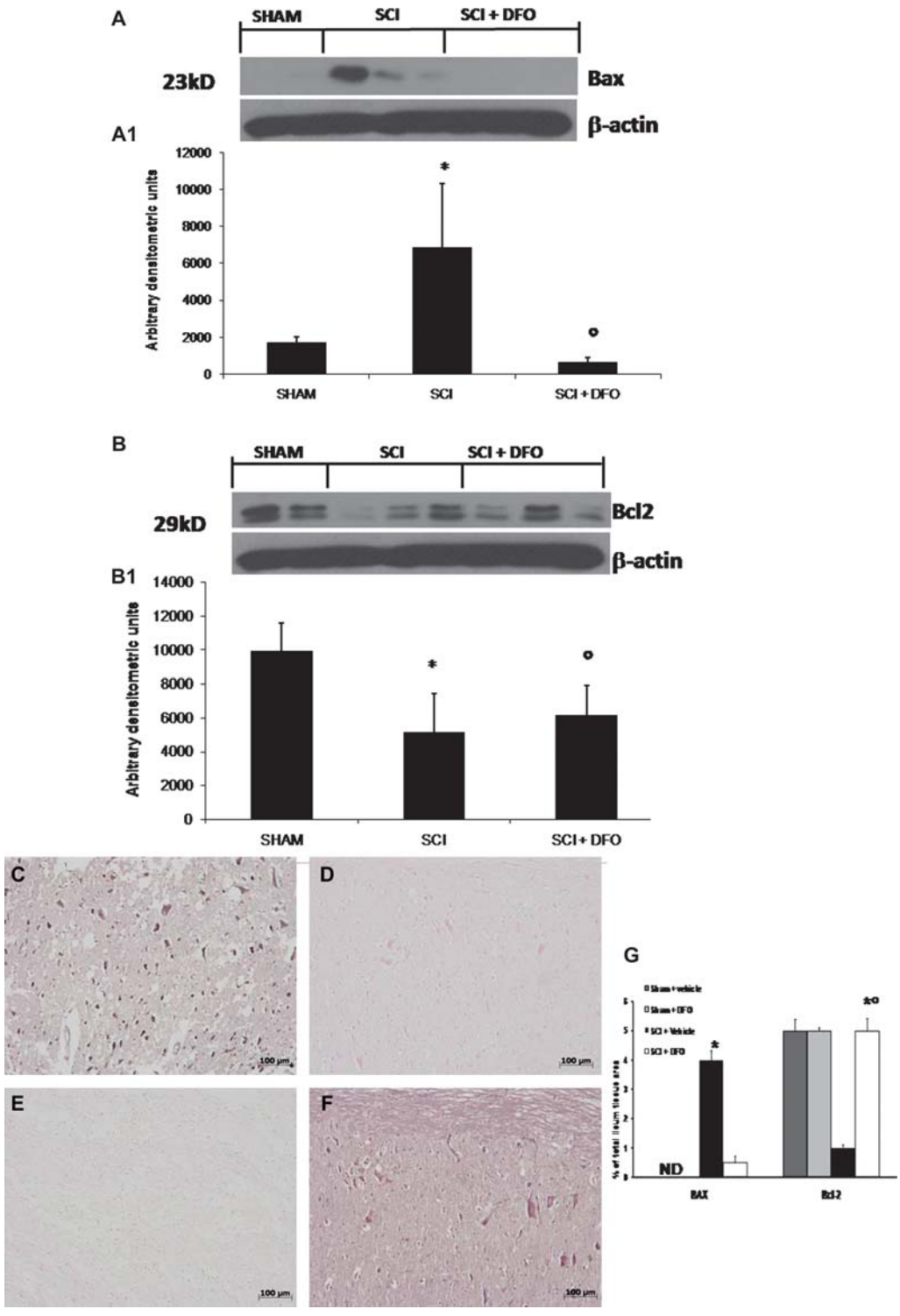


Figure 10. Western blot and immunohistochemical analysis for Bax and Bcl-2 expression. By Western blot analysis, Bax levels were appreciably increased in the spinal cord from SCI mice (A and A1). On the contrary, DFO treatment prevented SCI-induced Bax expression (A and A1). Moreover, a basal level of Bcl-2 expression was detected in spinal cord samples from sham-operated mice. Bcl-2 expression was significantly reduced in spinal cord samples from SCI mice (B and B1). DFO treatment significantly reduced the SCI-induced inhibition of Bcl-2 expression (B and B1). The results in (A1) and (B1) are expressed as mean ± SEM from $n = 5/6$ spinal cord for each group. $^{*}p < 0.01$ vs sham, $^{\circ}p < 0.01$ vs SCI + vehicle. Sections of spinal cord from SCI mice exhibited positive staining for Bax ©. DFO treatment reduced the degree of positive staining for Bax in the spinal cord of mice subjected to SCI (D). In addition, in the spinal cord sections from SCI control mice, the staining for Bcl-2 significantly reduced (E). DFO treatment attenuated the loss of positive staining for Bcl-2 in the spinal cord from SCI-subjected mice (F). Densitometry analysis of immunocytochemistry photographs ($n = 5$ photos from each sample collected from all mice in each experimental group) for Bax and for Bcl-2 (G) from spinal cord tissues was assessed. The assay was carried out by using Optilab Graftek software on a Macintosh personal computer (CPU G3-266). Data are expressed as a percentage of total tissue area. This figure is representative of at least three experiments performed on different experimental days. $^{*}p < 0.01$ vs Sham. $^{\circ}p < 0.01$ vs SCI + vehicle.

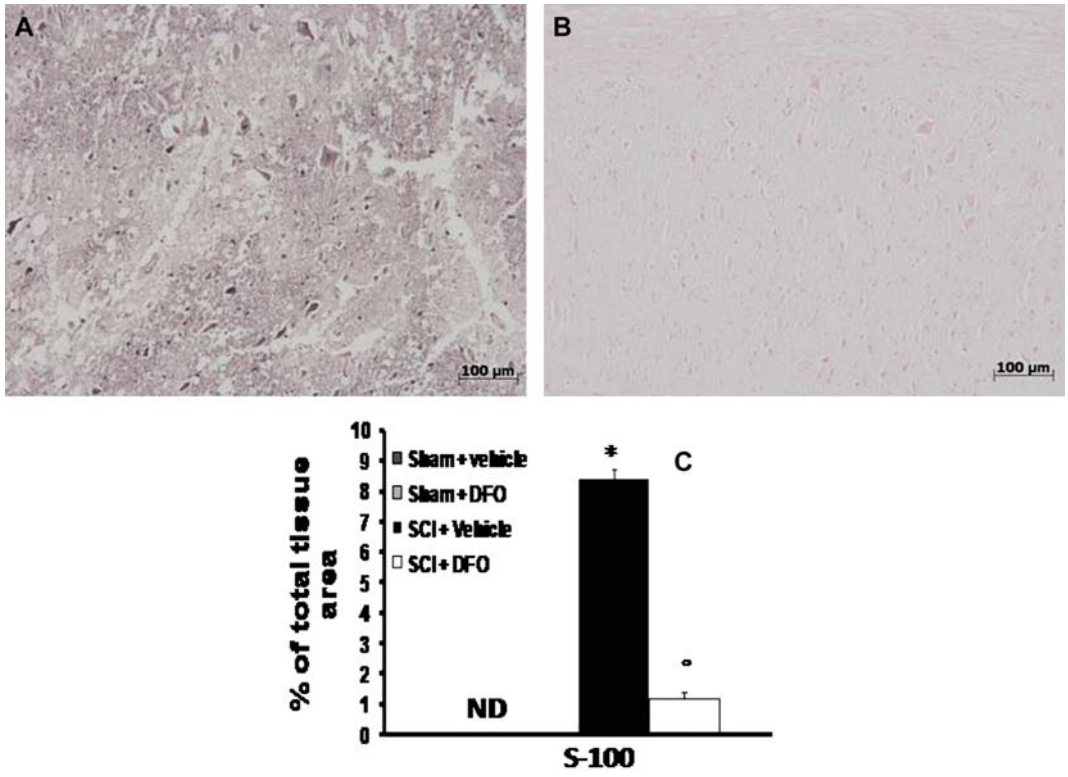


Figure 11. Effect of DFO on S-100 expression. Spinal cord sections were processed at 24 h after SCI to determine the immunohistological staining for S-100. A substantial increase in S-100 (A) expression was found in inflammatory cells, in nuclei of Schwann cells in the spinal cord tissues from SCI mice. Spinal cord levels of S-100 (B) were significantly attenuated in DFO-SCI treated mice in comparison to SCI animals. Densitometry analysis of immunocytochemistry photographs ($n=5$ photos from each sample collected from all mice in each experimental group) for S-100 (C) from spinal cord tissues was assessed. The assay was carried out by using Optilab Graftek software on a Macintosh personal computer (CPU G3-266). This figure is representative of at least three experiments performed on different experimental days. $^{*}p < 0.01$ vs Sham. $^{\circ}p < 0.01$ vs SCI+vehicle.

It's well known that two different apoptotic pathways can be activated after SCI. One of these is the death receptor pathway, characterized following binding of ligands to extracellular death receptors such as TNF receptor, CD95/Fas [38]. These receptors, after activation, recruit and activate in turn other proteins (like caspase 8, caspase 3 and others), leading at least to cleavage of several substrates, like cytoskeleton-associated proteins, transcription factors and proteins involved in DNA repair (PARP) and chromatin structure.

With the second pathway, the activation of caspases occurs through a mitochondrial mechanism [38]. Cytochrome *c* released from mitochondria into the cytosol binds with procaspase 9 and Apaf-1. This binding activates executioner caspases and initiates several events that overlap with those of the first pathway by death receptors. This way is modulated by members of the Bcl-2 family, proteins that localize to membranes, including mitochondrial membranes. Inside of this family group there is anti-apoptotic proteins Bcl-2 and Bcl-XL as well as the pro-apoptotic protein Bax.

Moreover various studies have postulated that Bax, a pro-apoptotic gene, plays an important role in developmental cell death and CNS injury [39]. Similarly, it has been shown that the administration of Bcl-xL fusion protein (Bcl-xL FP) (Bcl-2 is the most expressed anti-apoptotic molecule in adult central nervous system) into injured spinal cords significantly increased neuronal survival, suggesting that SCI-induced changes in Bcl-xL contribute considerably to neuronal death . Based on these evidences, we have identified in SCI pro-apoptotic transcriptional changes, including up-regulation of pro-apoptotic Bax and down-regulation of anti-apoptotic Bcl-2, by immunohistochemical staining. We report in the present study that the treatment with DFO in SCI experimental model documents features of apoptotic cell death after SCI, suggesting that protection from apoptosis may be a pre-requisite for regenerative approaches to SCI. In particular, we demonstrated that the treatment with DFO reduced Bax expression, while, on the contrary, Bcl-2 expressed much more in mice treated with DFO. Therefore, FasL plays a central role in apoptosis induced by a variety of chemical and physical insults. Recently, it has been pointed out that FasL signalling plays a central role in SCI [40]. We confirm here that SCI leads to a substantial activation of FasL in the spinal cord tissues, which likely contributes in different capacities to the evolution of tissues injury. In the present study, we found that DFO treatment led to a substantial reduction of FasL activation. However,

it is not possible to exclude that the anti-apoptotic effect observed after DFO it may be partially dependent on the attenuation of the inflammatory-induced damage. Further studies are needed in order to clarify these mechanisms.

Several publications have all shown an increased interest in the mechanisms of glial neurotrophic factors, such as basic fibroblast growth factor (bFGF, FGF-2) and S100β, in the injury-related events in the forebrain [41].

S100β is a $Ca+^{2}$-binding protein and it is widely distributed in the central nervous system (CNS), including the spinal cord [42], being found mainly in astrocytes. A possible involvement is known in post-injury events of S100β, because it promotes gliogenesis and angiogenesis and may also stimulate secretion of glial extracellular matrix molecules. What is the mechanism that regulates S100β expression in reactive astrocytes after injury is not known. The present study, using immunohistochemistry and densitometry analysis, characterized the changes in S100β in reactive astrocytes and microglia in the spinal cord after contusion lesion induced by the application of the vascular clip. We observed that in DFO treated mice the staining is more and significantly evident when compared with SCI-operated mice, while we observed no significant evidence of the presence of S100β in the sham group mice.

Finally, in this study we demonstrated that DFO treatment significantly reduced the SCI-induced spinal cord inflammatory reactions. The results of the present study enhance our understanding on the role of chelators to prevent the participation of iron in oxygen radical formation, to mitigate the oxidative stress damage resulting from ischemia/reperfusion, neurodegenerative disease, inflammation or chemotherapeutic drugs . In conclusion, DFO, for its protective effects, may be useful in the therapy of spinal cord injury, trauma and inflammation.



## Acknowledgements

We thank Carmelo La Spada for excellent technical assistance during this study, Caterina Cutrona for secretarial assistance and Valentina Malvagni for editorial assistance with the paper.

***Declaration of interest:*** This study was supported by a grant from IRCCS Centro Neurolesi 'Bonino-Pulejo', Messina, Italy (SC). The authors report no conflicts of interest. The authors alone are responsible for the content and writing of the paper.

## References

[1] Shapiro S, Borgens R, Pascuzzi R, Roos K, Groff M, Purvines S, Rodgers RB, Hagy S, Nelson P. Oscillating field stimulation for complete spinal cord injury in humans: a phase 1 trial. J Neurosurg Spine 2005;2:3–10.

[2] Samadikuchaksaraei A. An overview of tissue engineering approaches for management of spinal cord injuries. J Neuroeng Rehab 2007;4:15.

[3] Winkler T, Sharma HS, Gordh T, Badgaiyan RD, Stalberg E, Westman J. Topical application of dynorphin A (1-17) antiserum attenuates trauma induced alterations in spinal cord evoked potentials, microvascular permeability disturbances, edema formation and cell injury: an experimental study in the rat using electrophysiological and morphological approaches. Amino Acids 2002;23:273–281.

[4] Conti A, Cardali S, Genovese T, Di Paola R, La Rosa G. Role of inflammation in the secondary injury following experimental spinal cord trauma. J Neurosurg Sci 2003;47:89–94.

[5] Knoblach SM, Huang X, VanGelderen J, Calva-Cerqueira D, Faden AI. Selective caspase activation may contribute to neurological dysfunction after experimental spinal cord trauma. J Neurosci Res 2005;80:369–380.

[6] Liu JB, Tang TS, Xiao DS. Changes of free iron contents and its correlation with lipid peroxidation after experimental spinal cord injury. Chin J Traumatol 2004;7:229–232.

[7] Yu J, Guo Y, Sun M, Li B, Zhang Y, Li C. Iron is a potential key mediator of glutamate excitotoxicity in spinal cord motor neurons. Brain Res 2009;1257:102–107.

[8] Donfrancesco A, Deb G, Dominici C, Pileggi D, Castello MA, Helson L. Effects of a single course of deferoxamine in neuroblastoma patients. Cancer Res 1990;50:4929–4930.

[9] Olivieri NF, Brittenham GM. Iron-chelating therapy and the treatment of thalassemia. Blood 1997;89:739–761.

[10] Gu Y, Hua Y, Keep RF, Morgenstern LB, Xi G. Deferoxamine reduces intracerebral hematoma-induced iron accumulation and neuronal death in piglets. Stroke 2009;40: 2241–2243.

[11] Okauchi M, Hua Y, Keep RF, Morgenstern LB, Xi G Effects of deferoxamine on intracerebral hemorrhage-induced brain injury in aged rats. Stroke 2009;40:1858–1863.

[12] Sirin BH, Ortac R, Cerrahoglu M, Saribulbul O, Baltalarli A, Celebisoy N, I kesen I, Rendeci O. Ischaemic preconditioning reduces spinal cord injury in transient ischaemia. Acta Cardiol 2002;57:279–285.

[13] Mullane K. Neutrophil-platelet interactions and post-ischemic myocardial injury. Prog Clin Biol Res 1989;301:39–51.

[14] Ohkawa H, Ohishi N, Yagi K. Assay for lipid peroxides in animal tissues by thiobarbituric acid reaction. Anal Biochem 1979;95:351–358.

[15] Bethea JR, Castro M, Keane RW, Lee TT, Dietrich WD, Yezierski RP. Traumatic spinal cord injury induces nuclear factor-kappaB activation. J Neurosci 1998;18:3251–3260.

[16] Basso DM, Beattie MS, Bresnahan JC. A sensitive and reliable locomotor rating scale for open field testing in rats. J Neurotrauma 1995;12:1–21.

[17] Joshi M, Fehlings MG. Development and characterization of a novel, graded model of clip compressive spinal cord injury in the mouse: Part 2. Quantitative neuroanatomical assessment and analysis of the relationships between axonal tracts, residual tissue, and locomotor recovery. J Neurotrauma 2002;19:191–203.

[18] Joshi M, Fehlings MG. Development and characterization of a novel, graded model of clip compressive spinal cord injury in the mouse: Part 1. Clip design, behavioral outcomes, and histopathology. J Neurotrauma 2002;19:175–190.

[19] Nakamura T, Keep RF, Hua Y, Schallert T, Hoff JT, Xi G. Deferoxamine-induced attenuation of brain edema and neurological deficits in a rat model of intracerebral hemorrhage. J Neurosurg 2004;100:672–678.

[20] Boldt DH. New perspectives on iron: an introduction. Am J Med Sci 1999;318:207–212.

[21] Gerlach M, Ben-Shachar D, Riederer P, Youdim MB. Altered brain metabolism of iron as a cause of neurodegenerative diseases? J Neurochem 1994;63:793–807.

[22] Fleischer JE, Lanier WL, Milde JH, Michenfelder JD. Failure of deferoxamine, an iron chelator, to improve neurologic outcome following complete cerebral ischemia in dogs. Stroke 1987;18:124–127.
[23] Keberle H. The biochemistry of desferrioxamine and its relation to iron metabolism. Ann N Y Acad Sci 1964;119:758–768.
[24] Palmer C, Roberts RL, Bero C. Deferoxamine posttreatment reduces ischemic brain injury in neonatal rats. Stroke 1994;25:1039–1045.
[25] Porter JB. Deferoxamine pharmacokinetics. Semin Hematol 2001;38:63–68.
[26] Jessen KR, Mirsky R. Nonmyelin-forming Schwann cells coexpress surface proteins and intermediate filaments not found in myelin-forming cells: a study of Ran-2, A5E3 antigen and glial fibrillary acidic protein. J Neurocytol 1984;13:923–934.
[27] Ousman SS, David S. MIP-1alpha, MCP-1, GM-CSF, and TNF-alpha control the immune cell response that mediates rapid phagocytosis of myelin from the adult mouse spinal cord. J Neurosci 2001;21:4649–4656.
[28] Weiss G, Werner-Felmayer G, Werner ER, Grunewald K, Wachter H, Hentze MW. Iron regulates nitric oxide synthase activity by controlling nuclear transcription. J Exp Med 1994;180:969–976.
[29] Gulturk S, Kozan R, Bostanci MO, Sefil F, Bagirici F. Inhibition of neuronal nitric oxide synthase prevents iron-induced cerebellar Purkinje cell loss in the rat. Acta Neurobiol Exp 2008;68:26–31.
[30] Olas B, Nowak P, Kolodziejczyk J, Ponczek M, Wachowicz B. Protective effects of resveratrol against oxidative/nitrative modifications of plasma proteins and lipids exposed to peroxynitrite. J Nutr Biochem 2006;17:96–102.
[31] Endoh M, Maiese K, Wagner J. Expression of the inducible form of nitric oxide synthase by reactive astrocytes after transient global ischemia. Brain Res 1994;651:92–100.
[32] Sato K, Tashiro Y, Chibana S, Yamashita A, Karakawa T, Kohrogi H. Role of lipid-derived free radical in bleomycin-induced lung injury in mice: availability for ESR spin trap method with organic phase extraction. Biol Pharm Bull 2008;31:1855–1859.

This paper was first published online on Early Online on 7 April 2010.

[33] Emerit J, Beaumont C, Trivin F. Iron metabolism, free radicals, and oxidative injury. Biomed Pharmacother 2001;55:333–339.
[34] Szabo C, Virag L, Cuzzocrea S, Scott GS, Hake P, O'Connor MP, et al. Protection against peroxynitrite-induced fibroblast injury and arthritis development by inhibition of poly(ADP-ribose) synthase. Proc Natl Acad Sci USA 1998;95:3867–3872.
[35] Bao X, Wu G, Hu S, Huang F. Poly(ADP-ribose) polymerase activation and brain edema formation by hemoglobin after intracerebral hemorrhage in rats. Acta Neurochir 2008;105: 23–27.
[36] Wu J, Ohlsson M, Warner EA, Loo KK, Hoang TX, Voskuhl RR, Havton LA. Glial reactions and degeneration of myelinated processes in spinal cord gray matter in chronic experimental autoimmune encephalomyelitis. Neuroscience 2008;156: 586–596.
[37] Simonart T, Degraef C, Andrei G, Mosselmans R, Hermans P, Van Vooren JP, Noel JC, Boelaert JR, Snoeck R, Heenen M. Iron chelators inhibit the growth and induce the apoptosis of Kaposi's sarcoma cells and of their putative endothelial precursors. J Invest Dermatol 2000;115:893–900.
[38] Wilson MR. Apoptotic signal transduction: emerging pathways. Biochem Cell Biol 1998;76:573–582.
[39] Nesic-Taylor O, Cittelly D, Ye Z, Xu GY, Unabia G, Lee JC, Svrakic NM, Liu XH, Youle RJ, Wood TG, McAdoo D, Westlund KN, Hulsebosch CE, Perez-Polo JR. Exogenous Bcl-xL fusion protein spares neurons after spinal cord injury. J Neurosci Res 2005;79:628–637.
[40] Ackery A, Robins S, Fehlings MG. Inhibition of Fas-mediated apoptosis through administration of soluble Fas receptor improves functional outcome and reduces posttraumatic axonal degeneration after acute spinal cord injury. J Neurotrauma 2006;23:604–616.
[41] Barger SW, Van Eldik LJ, Mattson MP. S100 beta protects hippocampal neurons from damage induced by glucose deprivation. Brain Res 1995;677:167–170.
[42] Marks A, O'Hanlon D, Lei M, Percy ME, Becker LE. Accumulation of S100 beta mRNA and protein in cerebellum during infancy in Down syndrome and control subjects. Brain Res Mol Brain Res 1996;36:343–348.